

# Effect of chemical composition on microstructure and mechanical properties of laser weld metal of high-tensile-strength steel

Hiroyuki Sumi · Kenji Oi · Koichi Yasuda

Received: 17 November 2013 / Accepted: 16 July 2014 / Published online: 3 August 2014  
© International Institute of Welding 2014

**Abstract** Laser beam welding (LBW) and laser-arc hybrid welding are expected to be applied to welding of high-strength steel plates over 780 MPa, because they have advantages such as low distortion and a narrow heat-affected zone. This research examined the relationship between the chemical composition of high-strength steel plates and the microstructure and mechanical properties of the weld metal with the aim of improving the toughness of welded joints of high-strength steels by the LBW process. The results revealed that weld metal toughness is strongly dependent on the carbon (C) content of the steel plates, and excellent toughness can be obtained in weld metals with low C contents having an almost fully lower bainite structure without formation of slender martensite austenite constituent (MA). Based on these results, a guideline for appropriate alloying element design for high-strength steels for LBW was proposed, targeting mechanical properties of tensile strength  $\geq 980$  MPa and toughness  $vE_{-40\text{ }^{\circ}\text{C}} \geq 47$  J.

**Keywords** Laser welding · Weld metal · Microstructure · Toughness · Hardness · High-strength steels

## 1 Introduction

Laser beam welding (LBW) and laser-arc hybrid welding are low-heat input, low distortion, and high-accuracy welding processes, and have been proposed as potential alternatives to conventional arc welding methods, which have fatal problems when welding high-strength steels over 780 MPa grade

such as toughness reduction associated with large heat input, delayed hydrogen cracking, and poor fatigue strength of the welded joints [1–4]. To address these problems, Japan's New Energy and Industrial Technology Development Organization (NEDO) conducted a study on practical application of LBW and laser-arc hybrid welding technologies to 980 MPa grade high-strength steel plates as part of the National Project "Fundamental Studies on Technologies for Steel Materials with Enhanced Strength and Functions." The aim of that study was to develop a LBW or laser-arc welding process and weld metal design capable of achieving high strength and toughness in the laser weld metal. The target mechanical properties of the weld metal were tensile strength of more than 980 MPa and toughness  $vE_{-40\text{ }^{\circ}\text{C}} \geq 47$  J [5].

This paper reports the results of a systematic study on the effects of the chemical composition of high-strength steel plates on the microstructure and mechanical properties of the LBW weld metal. The optimum microstructure morphology for securing high toughness in the LBW weld metal of high-strength steels is discussed, and a guideline for the appropriate alloy design to satisfy the target mechanical properties is proposed.

## 2 Experimental procedure

### 2.1 Steel plates used and laser welding conditions

In this research, steel plates with different C contents and carbon equivalents  $C_{eq}$ -WES were used to investigate the weld metal microstructure and mechanical properties of the laser weld metal of high-strength steels. Table 1 shows the chemical compositions of the steel plates. The nine steels A1–A9 had three C levels (0.05, 0.10, 0.15 mass%) and various Mo contents in the  $C_{eq}$ -WES range of 0.43–0.55 mass%. The composition of steel A5 was modified

Doc. IIW-2504, recommended for publication by Commission IX "Behaviour of Metals Subjected to Welding."

H. Sumi (✉) · K. Oi · K. Yasuda  
Steel Research Laboratory, JFE Steel Corporation, Tokyo, Japan  
e-mail: h-sumi@jfe-steel.co.jp

**Table 1** Chemical compositions of steel plates used

Mark	C	Si	Mn	P	S	Ni	Mo	B	Others	Ceq-WES (mass%)
A1	0.06	0.25	1.44	0.001	0.001	1.21	0.20	0.0001	Cu, Cr, Nb, Ti added	0.43
A2	0.06	0.26	1.44	0.001	0.001	1.20	0.41	0.0001		0.48
A3	0.05	0.26	1.45	0.001	0.001	1.20	0.60	0.0001		0.53
A4	0.11	0.25	1.43	0.001	0.001	0.79	0.10	0.0001		0.44
A5	0.10	0.25	1.43	0.001	0.001	0.83	0.31	0.0001		0.49
A6	0.10	0.26	1.43	0.001	0.001	0.79	0.50	0.0001		0.53
A7	0.16	0.24	1.38	0.001	0.001	0.29	0.03	0.0001		0.46
A8	0.15	0.25	1.40	0.001	0.001	0.29	0.20	0.0001		0.49
A9	0.15	0.26	1.44	0.001	0.001	0.30	0.41	0.0001		0.55
A10	0.11	0.25	1.41	0.005	0.001	0.79	0.29	0.0030		0.49
A11	0.05	0.26	1.80	0.002	0.001	0.01	0.49	0.0001		0.53

$$\text{Ceq-WES} = \text{C} + \text{Si}/24 + \text{Mn}/6 + \text{Ni}/40 + \text{Cr}/5 + \text{Mo}/4 + \text{V}/14$$

by adding boron (B) to obtain steel A10, and the composition of steel A3 was modified by increasing Mn and reducing Ni to obtain steel of the composition A11. A10 was used to investigate the effect of B addition in improving the hardenability of the laser weld metal of high-strength steel. These steels were melted with a vacuum melting furnace in the laboratory, and specimen plates were produced by hot rolling. The oxidation layers on both sides were removed by mechanical grinding and the plates were finished to a thickness of 12 mm.

Full penetration melt runs were performed on the steel plates using a CO<sub>2</sub> laser under the welding conditions shown in Table 2. The laser power was 13 kW, and the welding speed was 0.8 m/min. As shielding gases, He was used for the surface side and Ar was used for the back side.

## 2.2 Test methods

The weld metals of the LBW joints were subjected to microstructural examination, Vickers hardness measurement, and Charpy impact tests.

For microstructure observation, nital-etched specimens were prepared, and their microstructures were observed with an optical microscope. The microstructures obtained after 2-stage etching and after Selective Potentiostatic Etching by Electrolytic Dissolution method (SPEED) were examined

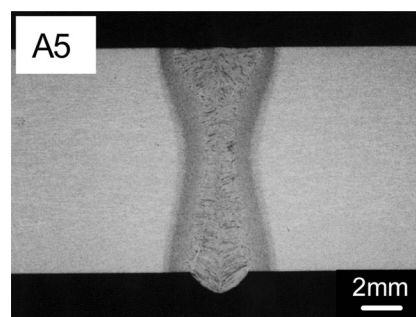
**Table 2** Laser welding conditions

Laser power	13 kW
Welding speed	0.8 m/min
Focal position	Surface of plate
Shielding gas	Surface: He (50 l/min) Back: Ar (10 l/min)

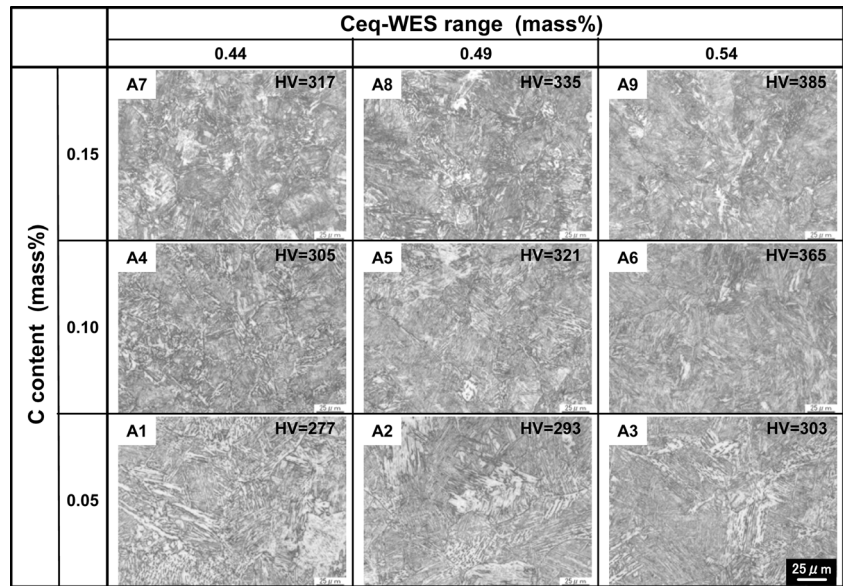
using a scanning electron microscope (SEM). The 2-stage etching was carried out to reveal the martensite austenite constituent (MA), and SPEED was performed to reveal carbides. In the 2-stage etching, 5 g ethylenediaminetetraacetic acid, 0.5 g NaF, and 100 ml distilled water were used in the first stage, and 25 g NaOH, 5 g picric acid, and 100 ml distilled water were used in the second stage [6]. The etchant used in SPEED was a 10 % acetylacetone, 1 % tetramethylammonium chloride, and methyl alcohol solution [7].

The Vickers hardness of the laser weld metal was measured at intervals of 0.5 mm in the cross-sectional thickness direction with a load of 9.8 N. The Charpy impact test was carried out using a standard 2 mm-V specimen notched at the center of the laser weld metal. The test temperature was −40 °C.

In this research, the chemical composition of the laser weld metal was assumed to be the same as that of the base metal, as the weld was prepared by remelting the base metal with the laser without using welding consumables.

**Fig. 1** Example of cross-section of laser weld (steel A5)

**Fig. 2** Microstructure change of laser weld metal influenced by C content and Ceq-WES of steel plates



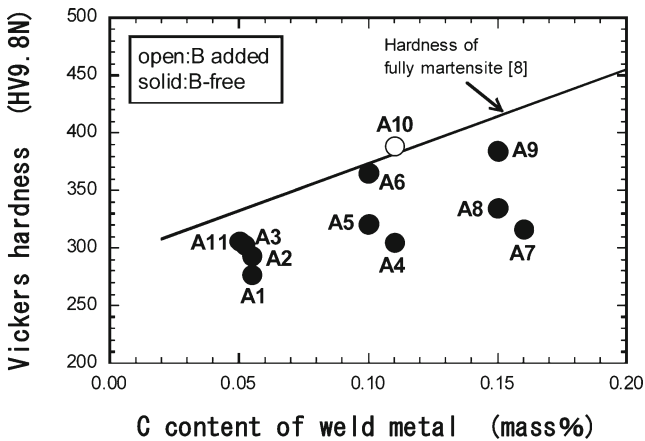
### 3 Results and discussion

#### 3.1 Influence of chemical composition on microstructure of laser weld metal

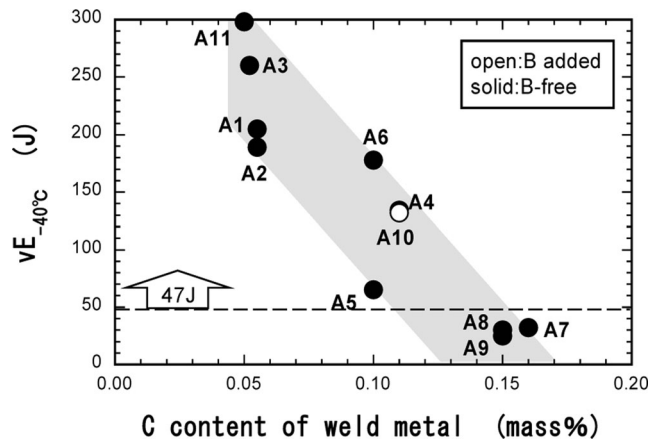
Figure 1 shows an example of a cross-sectional macrostructure of a full penetration laser weld. No significant differences were observed among the laser welds in this experiment, and no welding defects such as porosity and cracking were observed in any of the laser welds.

Figure 2 shows the influence of the C contents and Ceq-WES of the base metals on changes in the microstructures of the laser weld metals. Even steel A1, which had the lowest C content and Ceq-WES, displayed no formation of ferrite, either at the prior austenite grain boundary or within the grain. Hard structures of bainite and martensite were observed in all the laser weld metals, including A1.

Figure 3 shows the relationship between the C content and the Vickers hardness of the laser weld metal. The line in this figure is the correlation between the C content and the Vickers hardness of the fully martensite structure [8]. Judging from these results, the microstructure of the laser weld metal without B addition was considered not to be a fully martensite structure, but to be either a fully bainite structure or a bainite and martensite structure. However, with B addition, the microstructure was considered to be a fully martensite structure, as its high hardness corresponded to that of a fully martensite structure. As described in detail in Section 3.3, this study confirmed that the microstructure of the laser weld metal of A10 was mainly a martensite structure, demonstrating that B addition is effective in hardening the laser weld metal of high-strength steel.







**Fig. 3** Relationship between C content and Vickers hardness of laser weld metal



**Fig. 4** Effect of C content of laser weld metal on absorbed energy at -40 °C

**Fig. 5** Classification of bainite structure in this study

	Type <sup>[9]</sup>	Schematic diagram of bainite	Precipitation location of carbide
Upper Bainite	B <sub>I</sub>		No precipitation
	B <sub>II</sub>		Precipitation at the boundary of the bainitic ferrite
Lower Bainite	B <sub>III</sub>		Precipitation within the bainitic ferrite
	—		Precipitation within the planar ferrite

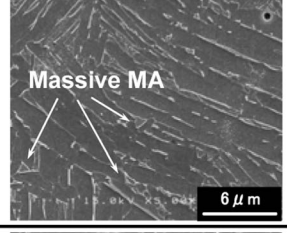
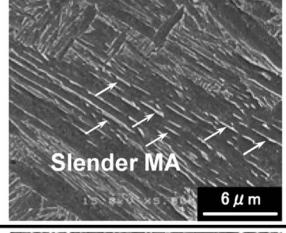
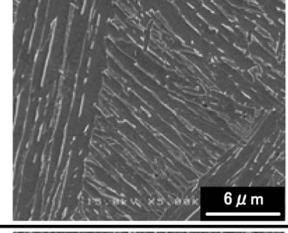
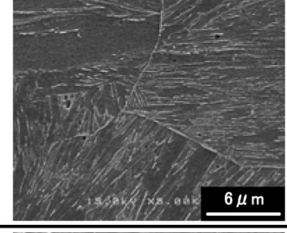
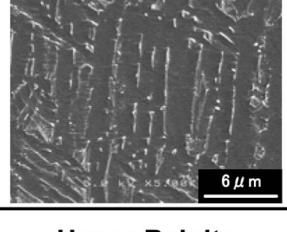
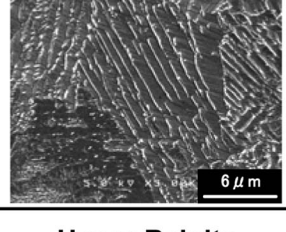
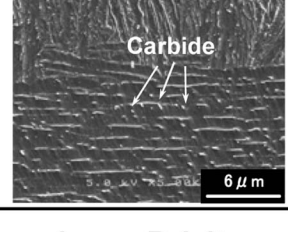
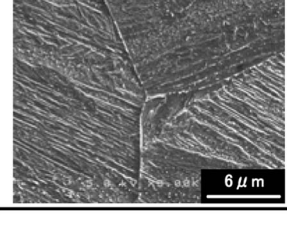
3.2 Influence of carbon content on toughness of laser weld metal

Figure 4 shows the effect of the C content on the toughness ( $vE_{-40\text{ }^\circ\text{C}}$ ) of the laser weld metal. The plots in this figure indicate the average of three test results. Absorbed energy  $vE_{-40\text{ }^\circ\text{C}}$  tends to decrease markedly with increasing C content. In other words, the toughness of the laser weld metal of high-strength steels is greatly affected by the C content. In particular, higher C contents caused the microstructure of the laser weld metal to change from lower bainite to martensite. Although lower bainite with a low C content is known to be a high toughness microstructure, martensite with a high C content has high hardness but low toughness. Therefore, laser

welding of high-tensile-strength steel with a high C content results in poor toughness of the weld metal.

3.3 Influence of microstructure on toughness of laser weld metal

Bainite structures are generally classified as either upper bainite or lower bainite. Two methods are used to classify bainite, one based on the shape of the bainitic ferrite and the other based on the precipitation location of the carbides in the bainitic microstructure [9, 10]. In this study, the bainite structures were classified by the precipitation location of the carbides, as shown in Fig. 5. Upper bainite was defined as a microstructure in which retained austenite and/or MA was

	A1 (HV=277, $vE_{-40\text{ }^\circ\text{C}}$ =205)	A7 (HV=317, $vE_{-40\text{ }^\circ\text{C}}$ =32)	A3 (HV=303, $vE_{-40\text{ }^\circ\text{C}}$ =260)	A10 (HV=389, $vE_{-40\text{ }^\circ\text{C}}$ =132)
2-stage etched microstructure				
SPEED etched microstructure				
	Upper Bainite (Massive MA)	Upper Bainite (Slender MA)	Lower Bainite + (Martensite)	Martensite

**Fig. 6** Comparison of 2-stage etching and SPEED etching microstructures of laser weld metal among A1, A3, A7, and A10



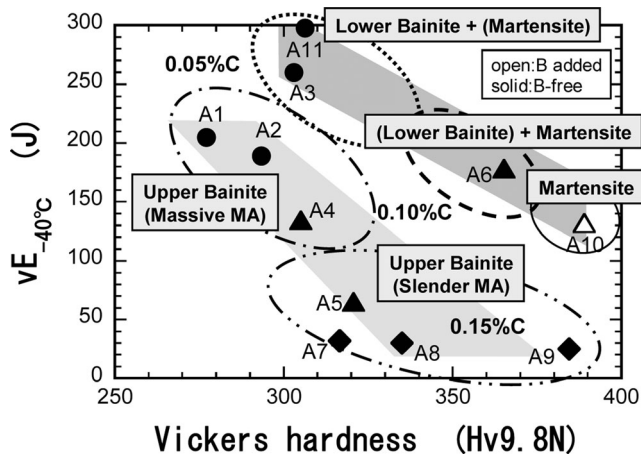


Fig. 7 Influence of microstructure on toughness and hardness of laser weld metal of high-strength steel

generated and a microstructure in which carbides were precipitated at the boundary of the bainitic ferrite. Lower bainite was defined as a microstructure in which carbides were precipitated within the bainitic ferrite.

Figure 6 shows examples of SEM images of the 2-stage etching microstructure and SPEED etching microstructure of the respective laser weld metal. First, in A1 (0.06 % C, Ceq-WES=0.43 %), the 2-stage etching microstructure revealed formation of massive MA between the lath structures, and carbides were not observed within the wide laths in the SPEED etching microstructure. From these results, A1 was considered to be an upper bainite structure containing massive MA. In the case of A7 (0.16 % C, Ceq-WES=0.46 %), much slender MA was observed among the laths in the 2-stage etching microstructure, and again, no precipitation of carbides was observed in the laths in the SPEED etching microstructure. From this, A7 was considered to be an upper bainite structure containing slender MA, and this steel displayed poor toughness. In contrast, in A3 (0.05 % C, Ceq-WES=0.53 %),

formation of MA was not observed in the 2-stage etching microstructure, but orientated precipitation of carbides was observed within the lath structure in the SPEED etching microstructure. These results indicated that A3 had an almost fully lower bainite structure, and as expected, steel A3 displayed the highest toughness among these weld metals. On the other hand, A10 (0.11 % C, B addition, Ceq-WES=0.49 %) did not display MA in the 2-stage etching microstructure, no carbides were observed in the lath structure in the SPEED etching microstructure, and the lath width was also very narrow. From these results, A10 was considered to be a fully martensite structure.

Figure 7 shows the hardness and toughness of the laser weld metals organized by the microstructural morphology. As a whole, absorbed energy  $vE_{-40\text{ }^{\circ}\text{C}}$  tends to decrease with increasing Vickers hardness. However, the correlation can be divided roughly into two groups corresponding to the upper bainite structure containing MA and the lower bainite and/or martensite structure without MA. Figure 7 clearly shows that the high-strength laser weld metal with a fully lower bainite structure without formation of slender MA displays excellent toughness, and even at the same hardness, an upper bainite structure containing slender MA displays remarkably poor toughness compared with a lower bainite structure.

### 3.4 Guideline for elemental design of laser weld metal for high-strength steel

Figure 8 shows the proposed guideline for the alloying element design of laser weld metal in order to satisfy the mechanical properties (tensile strength  $\geq 980$  MPa,  $vE_{-40\text{ }^{\circ}\text{C}} \geq 47$  J) which were the development target in this research. Here, the tensile strength of the weld metal was estimated using the value converted from the Vickers hardness. According to the hardness conversion table in SAE J417 released by the Society of Automotive Engineers (SAE), 980 MPa is equivalent to HV310. Therefore, weld metals having Vickers hardness of HV310 are considered to have an equivalent strength of 980 MPa in Fig. 8. Consequently, the C content should be controlled to less than 0.15 % to achieve high toughness, and the carbon equivalent Ceq-WES should be optimized to obtain the required strength. This guideline could also be applied to the laser-arc welding process by adjusting the chemical composition of the welding wire.

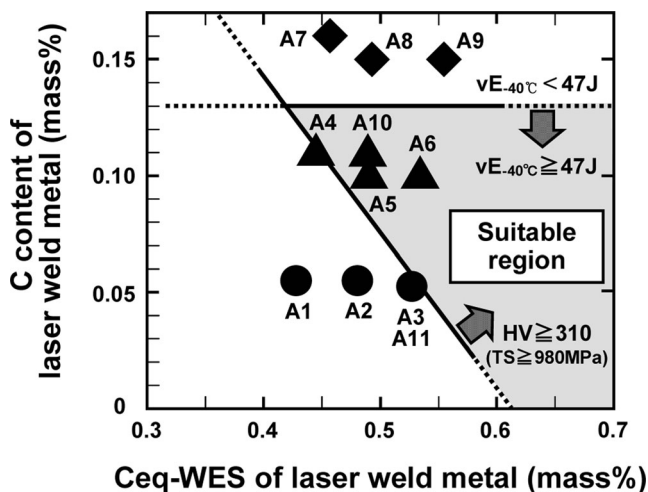


Fig. 8 Guideline for alloying element design of laser weld metal to achieve the target properties (tensile strength  $\geq 980$  MPa,  $vE_{-40\text{ }^{\circ}\text{C}} \geq 47$  J)

## 4 Conclusion

This paper described the relationship between the microstructure and mechanical properties of the laser weld metal of high-tensile-strength steels, with particular attention to the effect of

the chemical composition. The results of this research are summarized as follows.

- (1) Desirable toughness of  $vE_{-40\text{ }^{\circ}\text{C}} \geq 47$  J can be achieved in weld metals of high-strength steels having strength levels of 980 MPa by ensuring a fully lower bainitic microstructure with no MA constituent in the weld metal.
- (2) A guideline for the appropriate alloying element design of the laser weld metal of high-tensile-strength steels was proposed in order to achieve the target mechanical properties of tensile strength  $\geq 980$  MPa and  $vE_{-40\text{ }^{\circ}\text{C}} \geq 47$  J. According to this guideline, the C content should be controlled to less than 0.15 % to obtain the targeted high toughness, and  $C_{\text{eq}}\text{-WES}$  should be optimized to obtain the required strength level.

**Acknowledgment** This study was carried out as a part of research activities in the National Project “Fundamental Studies on Technologies for Steel Materials with Enhanced Strength and Functions” by the Consortium of The Japan Research and Development Center of Metals (JRCM). The financial support of Japan’s New Energy and Industrial Technology Development Organization (NEDO) is gratefully acknowledged. The authors also wish to express their deep appreciation to Dr. Tsukamoto of the National Institute for Materials Science (NIMS) for his generous cooperation in the production of the laser welded joints used in this research.

## References

1. Russell JD (2000) Laser weldability of C-Mn steels. *Weld World* 44–6:23–28
2. Kristensen JK (2001) Laser welding in ship building, a challenge to research and development for more than a decade. Proc. of 7th Int. Aachen Welding Conf. on High productivity joining processes - fundamentals, applications and equipment (iASTK 2001), Aachen
3. Kristensen JK (2002) Trends and developments within welding and allied process. IIW Int. Conf. advanced processes & technologies in welding & allied processes, Copenhagen
4. Koga H, Goda H, Terada S, Hirota K, Nakayama S, Tsubota S (2010) First application of hybrid laser-arc welding to commercial ships. *Mitsubishi Heavy Ind Tech Rev* 47–3:59–64
5. Nakanishi Y, Yamaoka H, Inose K, Yasuda K (2009) *Yousetu-Gizyutu* 57–11:54–59 (in Japanese)
6. Ikawa H, Oshige H, Tanoue T (1980) Effect of martensite-austenite constituent on the HAZ toughness of a high strength steel, IIW Doc. IX-1156-80
7. Kurosawa F, Taguchi I, Tanino M (1981) An application of the SPEED method (Selective Potentiostatic Etching by Electrolytic Dissolution) to the study of ferrous materials. *Bull Jpn Inst Met* 20–5:377–384 (in Japanese)
8. Terasaki T, Akiyama T, Serino M (1984) Chemical compositions and welding procedure to avoid cold cracking. Proc. Int. Conf. Joining and Metals, Helsingor, pp 381–386
9. Ohmori Y, Ohtani H, Kunitake T (1971) The bainite in low carbon low alloy high strength steels. *Trans ISIJ* 11:250–259
10. Bramfitt BL, Speer JG (1990) A perspective on the morphology of bainite. *Metall Trans A* 21A–3:817–829